The relationship between brain tumor cell invasion of engineered neural tissues and in vivo features of glioblastoma.

Zeynab Nayernia, Laurent Turchi, Erika Cosset, Hedi Peterson, Valérie Dutoit, Pierre-Yves Dietrich, Diderik Tirefort, Hervé Chneiweiss, Johannes-Alexander Lobrinus, Karl-Heinz Krause, et al.

Brain tumor cell invasion of engineered neural tissues mimics *in vivo* features of glioblastoma

Zeynab Nayernia[1], Laurent Turchi[6,7], Erika Cosset[2], Hedi Peterson[1], Valérie Dutoit[3], Pierre-Yves Dietrich[3], Diderik Tirefort[1,2], Hervé Chneiweiss[4], Johannes-Alexander Lobrinus[5], Karl-Heinz Krause[1], Thierry Virolle[6,7*], Olivier Preynat-Seauve[2*]

[1] Department of Pathology and Immunology, Faculty of Medicine, University of Geneva, CH-1211, Geneva, Switzerland

[2] Laboratory of immunohematology, Geneva University Hospital, CH-1211, Geneva, Switzerland

[3] Laboratory of tumor immunology, centre of oncology, Geneva University Hospital, CH-1211, Geneva, Switzerland

[4] INSERM U752, Faculty of Medicine, University of Paris Descartes, 75014 Paris, France

[5] Neuropathology Unit, Geneva University Hospital, CH-1211, Geneva, Switzerland

[6] Université de Nice-Sophia Antipolis, 06108, Nice, France

[7] Institut de Biologie Valrose, CNRS UMR 7277 – INSERM UMR1091, 06108 Nice, France

RUNNING HEADLINE

A new *in vitro* model of glioblastoma

*Corresponding authors:

Dr O. Preynat-Seauve, olivier.preynat-seauve@hcuge.ch,

Dr Thierry Virolle, virolle@unice.fr

*equal contribution

ABSTRACT

Glioblastoma is an aggressive brain tumor characterized by its high propensity for local invasion, formation of secondary foci within the brain, as well as areas of necrosis. This study aims to (i) provide a novel technical approach to reproduce features of the disease *in vitro* and (ii) characterize the tumor/host brain tissue interaction at the molecular level. Human Engineered Neural Tissue (ENT) obtained from pluripotent stem cells were generated and co-cultured with human glioblastoma-initiating cells. Within two weeks, glioblastoma cells invaded the nervous tissue. This invasion displayed features of the disease *in vivo:* a primary tumor mass, diffuse migration of invading single cells into the nervous tissue, secondary foci, as well as peritumoral cell death. Through comparative molecular analyses, this model allowed the identification of more than 100 genes that are specifically induced and up-regulated by the nervous tissue/tumor interaction. Notably the type I interferon response, extracellular matrix-related genes were most highly represented and showed a significant correlation with patient survival. In conclusion, glioblastoma development within a nervous tissue can be engineered *in vitro*, providing a novel and relevant model to study the disease and allows the identification of clinically-relevant genes induced by the tumor/host tissue interaction.

KEY WORDS

in vitro test, nerve tissue engineering, neural cell, stem cell

INTRODUCTION

Human gliomas account for more than 70% of all brain tumors and of these, glioblastoma is the most frequent and malignant histological type. The prognosis of glioblastoma is poor and fewer than 3% of glioblastoma patients are still alive 5 years after diagnosis. Glioblastoma is characterized by infiltrative growth into the surrounding healthy brain, leading to secondary foci formation. The dispersed glioblastoma cells are out of reach of surgery, chemotherapy and radiation. Thus, the tumor cannot be completely removed and these remaining invading tumor cells is thought to be responsible for the poor prognosis of glioblastoma (1).

In order to understand the biological aspects of glioblastoma development, several experimental models have been developed including derivation of glioblastoma cell lines, organotypic slices and animal models. A major breakthrough in glioblastoma research was the isolation of a subpopulation of cells with stem cell features, the Glioblastoma Initiating Cells (GIC), harboring long term self-renewal ability and the multipotency capacity to differentiate into other cell types and form heterogeneous spherical structures in suspension called gliomaspheres (2). These spheres could be differentiated in culture into cells that phenotypically resemble the tumor from the patient (3, 4) are used to study glioblastoma / brain interaction *in vitro* when co-cultured with rodent or human organotypic brain slices *in vitro* (5, 6) or after injection into the brain of immunocompromised mice *in vivo* (7). Although significant progress has been achieved by foregoing experimental models, the vast majority do not mimic the pathophysiological microenvironment of human glioblastoma.

In this study, we have developed and characterized a novel three dimensional -approach to imitate *in vitro* features of tumor/host nervous tissue interaction in an exclusively human environment. To achieve this goal, we used a nervous tissue engineering method developed previously (8) which allows the differentiation of human pluripotent stem cell into nervous

tissue by using air-liquid interface culture. By co-culturing glioblastoma stem-like cells on the engineered nervous tissue, we establish a human tissue sharing similarities with glioblastoma development in the brain environment. This includes diffuse invasion, formation of secondary foci and necrosis areas. Using expression profile analysis, this model allowed us to identify general alterations in gene expression upon interaction of tumor cells with non-tumoral brain tissue.

MATERIAL AND METHODS

Culture of undifferentiated ESC. The ESC cell line H1 was from WiCell Research Institute (Madison, WI, http://www.wicell.org). H1 was maintained in 80% Dulbecco's modified Eagle's medium (DMEM)/Ham's F-12 medium (F12), 20% Knockout serum replacement, 2 mM L-glutamine, 1% nonessential amino acids, 0.1 mM β-mercaptoethanol, and 10 ng/ml bFGF. Mouse embryonic fibroblasts were used as feeders and isolated from embryos of pregnant CF-1 mice (Charles River Laboratories, Wilmington, MA, http://www.criver.com). Fibroblasts were cultured in DMEM, 10% fetal bovine serum (FBS), and 1% penicillin/streptomycin. Feeders were mitotically inactivated by irradiation (45-50 Gy) before being seeded on a 0.1% gelatin-coated plate.

ESC-derived engineered neural tissue. It was performed as previously described (8), including some minor modifications. Briefly, ESC colonies were detached with type IV collagenase (1 mg/ml) and cultured in suspension in ultra-low attachment plates (Corning Costar, Acton, MA, http://www.corning.com/lifesciences) for 1 week in neural induction medium (DMEM/F12, N2 supplement (Gibco)) supplemented with 10µM phenazopyridine. Approximately 5-10 ESC-derived clusters were plated on a hydrophilic polytetrafluoroethylene (PTFE) membrane (6 mm diameter, 0.4 lm; BioCell-Interface, La Chaux-de-Fonds,

Switzerland, http://www.biocell-interface.com). This membrane was then deposited on a Millicell-CM (0.4 µm) culture plate insert designed for 6-well plates (Millipore, Billerica, MA, http://www.millipore.com). One milliliter of neural induction medium supplemented with 10 µM phenazopyridine (9) was added to each well under the membrane insert for differentiation.

Isolation and cultivation of gliomaspheres. Viable fragments of high-grade human glioblastoma were transferred to a beaker containing 0.25% trypsin in 0.1 mM EDTA solution containing and slowly stirred at 37°C for 30-60 minutes. In some isolation processes, 0.6 mg/ml papaine and 10 mg/ml DNase were used instead of trypsin/EDTA. Dissociated cells were plated in 75-cm2 tissue culture flasks plated at 2,500-5,000 cells per cm2) in DMEM/F-12 medium (1:1) containing the N2, G5, and B27 supplements (all from Invitrogen, Carlsbad, CA, http://www.invitrogen.com). After several passage clusters of adherent cells detach and form spheres in different size in low attachment flasks (Corning Costar, Acton, MA, http://www.corning.com/lifesciences).

Immunohistochemistry. Immunohistochemistry analyses were carried out according to standard protocols. Briefly, samples were fixed in 4% paraformaldehyde in Dulbecco's BPS for 30 minutes at room temperature. The tissue was then fixed into selected agar gelatine for easier handling and embedded into paraffin. Sections (10 µm) were prepared with microtome deparaffinised and rehydrated. Slides were then incubated in citrate buffer (620-W microwave) for 15 minutes (0.01 M; pH 6.0) followed by three washes with PBS and incubated with appropriate dilutions of primary antibodies in PBS containing 0.3% Triton X-100 overnight at 4°C. After several washes in PBS, the sections were incubated with a secondary biotinylated antibodies and ABC reagent solution for 1 hour, separately (Vector laboratories,

http://*www.vectorlabs.com*). Colour was developed with 3, 3'-diaminobenzidine (DAB, Sigma-Aldrich) incubation for 10-20 minutes.

Antibodies. The following primary antibodies against human antigens were used: rabbit anti-cleaved caspase-3 (Cell Signaling Technology,Beverly, MA, http://www.cellsignal.com), rabbit anti-Musashi-1, rabbit anti-nestin, mouse anti-vimentin, rabbit anti-Sox-2 (all from Chemicon,Temecula, CA, http://www.chemicon.com), rabbit anti-glial fibrillary acidic protein (anti-GFAP) (all from Dako, Glostrup, Denmark, http://www.dako.com), mouse anti-βIII-tubulin (Sigma-Aldrich, St.Louis, http://www.sigmaaldrich.com), rabbit anti-α crystallin B (from Abcam, http:www.abcam.com).

RNA isolation. Isolation of total RNA was performed by using RNeasy mini kit from Qiagene following the manufacturer's protocol. RNA quality was verified by 2100 Bioanalyzer (Agilent) and the concentration was determined by the ND-1000 Spectrophotometer (NanoDrop).

Microarray. For each condition, 255 ng of total RNA was used to synthesize cRNA using the Illumina TotalPrep RNA amplification kit (Ambion). cRNA concentration was measured with a spectrophotometer and cRNA quality was determined by 2100 Bioanalyzer (Agilent). For microarray 750 ng of amplified cRNA product was hybridized to human HT-12 v4.0 Illumina micro arrays (Illumina) according to the manufacturer's instructions. Microarray preprocessing was done using R (R Development Core Team, 2011) and BioConductor packages. Microarrays were normalized and differentially expressed genes were identified using Limma package. Probes having FDR corrected p-values less than 0.05 and fold change larger than 2.5 between compared conditions were considered significantly differentially expressed. Each such gene set

ordered by fold change was characterized by Gene Ontology terms, KEGG and Reactome pathways, TRANSFAC binding predictions, MicroCosm miRNA sites, BIOGRID interaction data, human disease genes from Human Phenotype Ontology using g:Profiler webtool (default settings).

Q-PCR. Isolation of total RNA was performed by using RNeasy mini kit from Qiagene following the manufacturer's protocol. RNA concentration was assessed by nanodrop and 500 ng of total RNA was used to synthesize cDNA by using TAKARA kit following the manufactures protocol. Primer sequences were designed by Invitrogen primer design tools and are summarized in table 3. RT-PCR was carried out in optical 384-well plates and labeled by using the SYBR green master mix (Applied Biosystems), and the fluorescence was quantified with a Prism 7900 HT sequence detection system (Applied Biosystems). The expression of MX1, OAS1-3, IFIT-3, ISG15, C1QB, DHX58 genes was examined in a total volume of 10 _l containing 1_ SYBR green reagent, 0.86 μM of each gene-specific primer pair, and 1 ng of cDNA. For amplification the program recommended by Applied Biosystems was used (50°C for 2 min, 95°C for 10 min, 40 cycles of 95°C for 15 s and 60°C for 1 min). The relative level of each RNA was normalized to the corresponding Gapdh RNA levels. All TaqMan RT–PCR reactions were carried out in technical and biological triplicates, and the average cycle threshold (CT) values were determined.

Survival analysis. We performed survival analysis as a function of gene expression data. We used 518 normalized glioblastoma samples from The Cancer Genome Atlas (TCGA, downloaded 11.02.2013) for 10113 genes that overlap between the TCGA and our Illumina dataset. We created single gene models using Cox Proportional Hazards regression models with coxph routine from Survival package in R. Genes were considered affecting survival if the

coxph Wald test FDR corrected p-value was smaller than 0.05. Out of the 10113 genes 349 have an effect with a p-value smaller than the threshold (1807 before FDR correction). We concentrated our analysis on genes that are up-expressed in ENT+GIC compared to ENT. We studied further genes that had fold change above 2.5. There were 132 such Illumina probes that corresponded to 115 unique gene identifiers, out of which 97 are present in TCGA dataset. Out of these 97 genes, 148 have Wald test FDR correction p-value smaller than the threshold of 0.05 and were considered affecting patient survival. Such proportion of genes affecting survival is highly significant by a hypergeometric test p-value of 6.12e-10. We also did random sampling where we picked 100000 times 100 genes out of all the genes being present both in our and TCGA dataset to validate the significance of our results. The median number of genes affecting survival for a group of 100 random genes is 34 and the highest value we achieved from random sampling was 15, all clearly showing that our results are occurring more often than expected by random.

RESULTS

The initial goal of this study was the *in vitro* generation of a human glioblastoma-like tissue. Glioblastoma Initiating Cells (GIC) were isolated from surgically removed glioblastoma and maintained in culture as described in *material and methods*. These cells were able to form gliomaspheres in suspension when maintained in low attachment plates (Figure 1A). We first addressed if a differentiation program into a tumor-like tissue could be reproduced *in vitro*. For this, an air-liquid interface culture method we described previously was used to differentiate GIC (8). 15-20 gliomaspheres were placed on a polytetreafluoroethylene (PTFE) membrane and maintained for two weeks in neural induction medium. Once gliomaspheres were plated (Figure 1B), the spheres merged rapidly and formed a compact cell mass after 24h (Figure 1C).

As we described previously for neural stem cells, after two weeks of culture, a three dimensional tissue was obtained (8). Hemalun-eosin coloration of tissue sections revealed histological features similar to the tumor *in vivo* such as pleiomorphic nuclei, indistinct cytoplasmic borders and a distinct fibrillary cytoplasm (Figure 1D). Immunohistochemical staining revealed expression of neural and glial and markers found in glioblastoma including nestin, βIII-tubulin, Glial Fibrillary Acidic Protein (GFAP) and vimentin (Figure 1 E, F). cDNA microarray was performed and gene expression profile was compared for all genes before and after 2 weeks culture of gliomaspheres on air/liquid interface. The most important transcription changes after culture were observed for the group of proliferation-associated genes which displayed decreased expression (blue dots, Supplementary Figure 1). Genes involved in host defense such as interferon-responsive genes were not modified. Together, this suggests that air/liquid interface culture of human gliomaspheres generate a compact tissue. Compared to GIC before culture, this tissue acquires histological and phenotypical features similar to the tumor *in vivo*.

In order to mimic the *in vivo* environment, we sought to analyse GIC differentiation in the presence of an engineered human brain-likes tissue. As a source of brain-like tissue, human pluripotent stem cells were differentiated towards Engineered Nervous Tissues (ENT), accordingly to the method we described previously (8). For this purpose, GIC stably transduced with Tomato Fluorescent Protein (TFP) were seeded on the top surface of embryonic stem cells-derived ENT and maintained in culture for additional two weeks (Figure 2A). Two weeks after co-culture, area of TFP-positive cells had increased on the ENT, indicating gliomasphere survival and development in co-culture conditions (Figure 2B). TFP-positive area exhibited progressively a heterogeneous morphology (figure 2C) and some red fluorescent cells acquired a more mature morphology in favour of differentiation (Figure 2D). In addition, foci of individual TFP positive cells were observed in the ENT at distance of the main fluorescent area, suggesting that cells had migrated outside the initial implanted gliomaspheres (figure 2E).

Histological coloration with hemalun-eosin on tissue sections revealed a distinct area with appearance of neural tissue derived from embryonic stem cells (8) and regions with the characteristic morphology of glioblastoma (Figure 2F). Moreover, the tumor area expressed neural and glial markers reported in glioblastoma patients, such as nestin, GFAP, vimentin, Musashi-1 and Sox-2 (Figure 2 G-K).

Because massive invasiveness is one of the main characteristic of glioblastoma, we next sought to examine the infiltration and migration capability of gliomasphere into ENT. Since gliomaspheres were stably transfected to constitutively express TFP, it was possible to track cell infiltration into the ENT. Histological tissue section analysis by fluorescent microscopy confirmed the invasion process by the presence of numerous TFP-positive single cells infiltrating ENT (Figure 3A). This invasion was further confirmed by immunohistochemical analysis with the astrocytic marker GFAP (data not shown). In order to monitor the invasion path of gliomaspheres after co-culture, sections were prepared at different time points. Three days after gliomasphere plating on ENT, GFAP positive cells were at the surface of the tissue. After 6 and 9 days, GFAP positive cells started to migrate massively into the ENT (Figure 3B). This observation confirmed the capacity of gliomaspheres to massively invade and develop within their host tissue in the *in vitro* culture system.

Beside invasion into surrounding tissue, glioblastoma cells migrate at a distance and form secondary foci. A low magnification allowed detection of TFP-positive single cells at distance from the initial implanted glioblastoma (Figure 3C) and secondary tumor foci at the edges of the ENT (Figure 3D). Additionally, the tumor part of the co-culture tissue sections was immunoreactive for α-crystallin B (figure 3E) which is expressed by invading glioblastoma cells (10). Another important histological feature of glioblastoma is the presence of extensive cell death areas surrounding the tumor (11). Accordingly, large zones of cell death (Figure 3F,

picnotic and condensed nuclei) along with immunoreactivity for cleaved caspase 3, a marker for apoptosis, were observed within zones surrounding the tumor (Figure 3G).

In order to assess the development and infiltration capacity of an unrelated tumor, we used a similar strategy with the breast carcinoma cell line MCF-7 (12) and the MZ2-mel3.1 melanoma cell line. All the tumor cells were transduced with TFP for better visualization and spheres were formed in low attachment plates. Afterwards, TFP-positive spheres were co-cultured with ENT for two weeks (Figure 4A). Presence of TFP-positive cells (figure 4B) and their immunoreactivity for cytokeratins, a commonly used molecule to identify breast carcinoma (Figure 4C and D) confirmed the MCF-7 sphere survival and growth in the co-culture with ENT. Unlike the invasion and development path observed for glioblastoma, few single cell invasion and absence of secondary foci away from the initial implanted MCF7 spheres on ENT could be detected. Although TFP-positive MZ2-mel3.1 melanoma cells survived after two weeks of co-culture on ENT, most of the cells did not remained on the surface ENT and moved to the periphery of ENT and did not infiltrate the host tissue (Figure 4E). Finally, gliomaspheres derived from other surgically removed glioblastoma were evaluated for their ability to survive and develop within ENT (Supplementary table 1). Although some gliomaspheres showed low development within ENT (e.g. TG6) most of them had the capacity to develop and infiltrate ENT. Altogether, these observations show that co-culture of gliomaspheres within ESC-derived neural tissue recapitulates some of the important histological features of glioblastoma development in patients.

The invasion and migration of glioblastoma into the adjacent healthy brain tissue has been known to be involved with molecular changes. To provide insight into the gene expression pattern elicited in our co-culture system, we performed a comparative cDNA microarray study. Accordingly, whole RNA was extracted and entire transcriptoma were analyzed in three biological replicates using the following conditions: (I) gliomaspheres before differentiation on

air/liquid interface, (II) gliomaspheres after differentiation on air/liquid interface, (III) ENT and (IV) gliomaspheres cocultured with ENT (Figure 5A). For this experiment, we selected the gliomasphere GB1 for its high invasion rate as compared to other gliomaspheres tested. Fold change analysis between ENT+tumor and ENT alone or tumor alone was performed to detect differentially expressed genes. Transcriptional changes were observed between the different conditions. Notably, the gene expression profile of the ENT+tumor condition significantly differed from the ENT alone or tumor alone condition, suggesting that the host/tumor interaction is associated with transcriptional changes (figure 5B). In order to understand what is the most represented family of up-regulated genes, functional annotation was performed using g: Profiler software (13, 14). This analysis showed that the majority of induced/up-regulated genes in the condition ENT+tumor belongs to the type I interferon signaling cascade (GO:0071357 – cellular response to type I interferon). These regulatory genes involved in host defense have been described to be downstream targets of the interferon/STAT1 signaling cascade (15). Scatterplot demonstrates multiple genes linked to the type I IFN pathway are up-regulated in ENT+tumor condition compared to tumor alone ENT alone (Figure 5C and 5D respectively, red dots) (Full list of genes in Supplementary File 2 and 3).

To confirm these observations, a panel of selected type I IFN-related genes with the highest fold change was tested by regular quantitative PCR. For this, a similar comparative experiment was repeated followed by relative expression analysis of gene candidates (Figure 6A). Similar co-culture experiments were performed with tumor spheres from glioblastomas as well as an unrelated tumor (breast carcinoma MCF-7) (figure 6B). Up-regulation of type I IFN related genes was confirmed in glioblastoma but not in MCF-7 co-cultured with ENT. Thus, the interaction between glioblastoma and host nervous tissue allows by itself the induction of transcriptional changes. The most important response was the induction of type I-interferon-related genes. Accordingly, previous studies have reported that type I interferon-related genes

play a role in glioblastoma. Studies show that their expression signature can be exploited to predict glioblastoma patient's survival (15). In addition these genes have been identified as predictor of glioblastoma resistance to radiation therapy (16).

To further understand the clinical significance of the changes in gene expression, we compared our results to data from the TCGA (The Cancer Genome Atlas TCGA) dataset. The TCGA provides data on the correlation between gene expression data of glioblastoma samples and related patient mortality information. We first concentrated our analysis on genes that are significantly up-regulated in ENT+tumor as compared to ENT alone (2.5 fold change; Figure 7A, left side of the panel). A total of 97 genes that were also present in the TCGA data set were found to fit this criterion. Interestingly, three quarters of these genes (73) fell into three functional groups: interferon response-related genes (42), extracellular matrix-related genes (25), and cholesterol-related genes (6). On the right side of Figure 7A, the effect of tumor expression of these genes on patient mortality (as provided by TCGA) is given. Interferon and extracellular matrix-related genes that were up-regulated in our *in vitro* system, showed - in many instances - a high impact on patient mortality. However, this did not seem to be the case for genes related to cholesterol metabolism.

To investigate whether enrichment of genes with impact on patient survival in the *in vitro* system could have been a random event, we compared our results to the ratio calculated both from randomly selected genes and from gene group having similar but not significant expression changes (for details see also the material and methods section). Figure 7B shows the results of this analysis. Genes having been identified in our *in vitro* assay as significantly changes are shown in orange (significant up-regulation) or turquoise (significant down-regulation), while the randomly selected genes are shown in grey. On the X-axis genes were aligned by their fold change in the *in vitro* assay (increased expression on the left and decreased expression on the right). The Y-axis shows the percentage of genes with impact on patient

mortality (as calculated from TCGA data). Visual inspection shows that sampling of genes up-regulated in the *in vitro* assay yielded an increased percentage of genes having an impact on patient mortality. Out of these 97 genes that were significantly up-regulated in the *in vitro* assay, 148 have Wald test FDR corrected p-value smaller than the threshold of 0.05 and were considered affecting patient survival. Such proportion of genes affecting survival is highly significant by a hypergeometric test p-value of 6.12e-10. We also did random sampling where we picked 500 000 times 100 genes out of all the genes being present both in our and TCGA dataset to validate the significance of our results. The median number of genes affecting survival for a group of 100 random genes was 34 and the highest value we achieved from random sampling was 15. Thus, gene up-regulation *in vitro* identified a significant proportion of genes that have an impact on patient survival (Full list of the genes available in Supplementary File 4).

DISCUSSION

Extensive infiltration of normal brain tissue by individual cancer cells and peritumoral cell death is histological hallmark of glioblastoma, yet experimental approaches to study these phenomenons in a fully human model are limited. In this study we have developed an easily available *in vitro* tool, which reproduces these features and allows identification of a gene signature, specifically induced upon tumor/host tissue interaction, similar to the molecular signature observed in glioblastoma patients. Among these genes, a group related to interferon response (18-20) and extracellular matrix (21, 22) were most highly represented and correlated with tumor aggressiveness

The tissue engineering approach described in this study provides an attractive combination of multiple advantages to study the disease *in vitro*. The engineered tissue

organization provides a direct tumor / host tissue interaction. These advantages are also provided by animal models and organotypic slices but, the tissue engineering approach also offers the benefit of the human origin of the different counterparts (tumor and host tissue), increasing the predictive value of experimental observations. Another benefit is the potential to repeat experiments due to the availability of tissue provided by the use of stem cells. In contrast to animal models, the tissue engineering approach does not include the presence of vessels and immune cells. As angiogenesis and immune response actively contribute to disease progression (23, 24), introduction of endothelial progenitors as well as cells of the leukocyte lineage (e.g. hematopoietic stem cells, tumor-infiltrating leukocytes) should be performed to come closer to the tumor *in vivo*.

The possibility to experimentally introduce or delete genes within the tumor and/or host tissue is particularly attractive for the development of innovative drug screening assays. In addition, reporter constructs such as luciferase could be used in order to quantify the tumor cells number versus ENT to ensure specific drug targeting of the tumor tissue. The successful development of such an approach would provide an attractive tool for drug discovery approaches based on library screening.

One of the new aspects of this study is the massive transcriptional change observed solely upon interaction of glioblastoma cells with adjacent nervous tissue. Indeed, over 100 genes were either repressed or significantly up-regulated upon tumor/host tissue interaction. Obviously, when taking tumor tissues from patients, there are differences in gene expression as compared to healthy brain tissue. However, this can simply be explained by different gene expression in tumor cells, by infiltration of tumor tissue with inflammatory cells, or by gene expression due to angiogenesis. None of the latter applies to the genes identified in our study because there are no inflammatory and no angiogenic cells in our system. More importantly, baseline gene expression in both tumor cells and native tissues was analyzed. Thus, this model

has the advantage to allow identification of genes which are exclusively regulated by tumor/ host tissue interaction. Importantly the identified genes correspond to a glioblastoma signature, both in terms of tumor biology and in terms of epidemiologically documented effects, thus validating the relevance of this model. Of these, up-regulated genes in response to tumor/nervous tissue interaction, the majority fell into 3 groups: type I interferon response, extracellular matrix and cholesterol-related genes. In tumor samples, up-regulation of genes related to the interferon-response has been documented and associated with poor patient outcome (16, 17, 20). Similarly, extracellular matrix and cholesterol metabolism subsets are all related to either glioblastoma directly or tumor invasion in general (25).

CONCLUSION

In this study, we have provided evidence that the co-culture of glioblastoma stem-like cells with an engineered three dimensional neural tissue, offers a novel way to study human glioblastoma *in vitro*. Our results show that important cellular and molecular features of human glioblastoma can be reproduced *in vitro*. These findings reinforce the concept of tissue engineering for the study of tumor/host tissue interaction. In the future, this may provide not only a powerful tool for the study of tumor development, but could also be optimized for large scale screenings of anti-cancer drugs.

.

AKNOWLEDGMENTS

Authors thank Dr Stefano Mandriota for the gift of MCF7 cell lines. This work was granted by the 3R research foundation (to O.P. S and T.V.), the ARTERES foundation (to O. P.S), the ISREC foundation (to O.P.S.), the Egon Naef Foundation (to O.P.S.), the *association*

pour la recherche sur le cancer (grant number 3161) (to T.V.), the association *Sauvons Laura (to T.V.),* Agence Nationale pour la Recherche ANR (GLIOMIRSTEM project) (to T.V.).

REFERENCES

1. Dunn GP, Rinne ML, Wykosky J, Genovese G, Quayle SN, Dunn IF, et al. Emerging insights into the molecular and cellular basis of glioblastoma. Genes & development. 2012;26(8):756-84. Epub 2012/04/18.

2. Binda E, Visioli A, Reynolds B, Vescovi AL. Heterogeneity of cancer-initiating cells within glioblastoma. Front Biosci (Schol Ed). 2012;4:1235-48. Epub 2012/06/02.

3. Das S, Srikanth M, Kessler JA. Cancer stem cells and glioma. Nature clinical practice Neurology. 2008;4(8):427-35. Epub 2008/07/17.

4. Singh SK, Clarke ID, Terasaki M, Bonn VE, Hawkins C, Squire J, et al. Identification of a cancer stem cell in human brain tumors. Cancer research. 2003;63(18):5821-8. Epub 2003/10/03.

5. Guerrero-Cazares H, Chaichana KL, Quinones-Hinojosa A. Neurosphere culture and human organotypic model to evaluate brain tumor stem cells. Methods Mol Biol. 2009;568:73-83. Epub 2009/07/08.

6. Ohnishi T, Matsumura H, Izumoto S, Hiraga S, Hayakawa T. A novel model of glioma cell invasion using organotypic brain slice culture. Cancer research. 1998;58(14):2935-40. Epub 1998/07/29.

7. Brehar FM, Ciurea AV, Chivu M, Zarnescu O, Radulescu R, Dragu D. The development of xenograft glioblastoma implants in nude mice brain. J Med Life. 2008;1(3):275-86. Epub 2008/07/01.

8. Preynat-Seauve O, Suter DM, Tirefort D, Turchi L, Virolle T, Chneiweiss H, et al. Development of human nervous tissue upon differentiation of embryonic stem cells in three-dimensional culture. Stem Cells. 2009;27(3):509-20. Epub 2008/12/17.

9. Suter DM, Preynat-Seauve O, Tirefort D, Feki A, Krause KH. Phenazopyridine induces and synchronizes neuronal differentiation of embryonic stem cells. J Cell Mol Med. 2009;13(9B):3517-27. Epub 2010/03/04.

10. Goplen D, Bougnaud S, Rajcevic U, Boe SO, Skaftnesmo KO, Voges J, et al. alphaB-crystallin is elevated in highly infiltrative apoptosis-resistant glioblastoma cells. The American journal of pathology. 2010;177(4):1618-28. Epub 2010/09/04.

11. Kim JH, Bae Kim Y, Han JH, Cho KG, Kim SH, Sheen SS, et al. Pathologic diagnosis of recurrent glioblastoma: morphologic, immunohistochemical, and molecular analysis of 20 paired cases. The American journal of surgical pathology. 2012;36(4):620-8. Epub 2012/03/24.

12. Lin NU, Bellon JR, Winer EP. CNS metastases in breast cancer. Journal of clinical oncology : official journal of the American Society of Clinical Oncology. 2004;22(17):3608-17. Epub 2004/09/01.

13. Reimand J, Kull M, Peterson H, Hansen J, Vilo J. g:Profiler--a web-based toolset for functional profiling of gene lists from large-scale experiments. Nucleic acids research. 2007;35(Web Server issue):W193-200. Epub 2007/05/05.

14. Cheon H, Yang J, Stark GR. The functions of signal transducers and activators of transcriptions 1 and 3 as cytokine-inducible proteins. Journal of interferon & cytokine research : the official journal of the International Society for Interferon and Cytokine Research. 2011;31(1):33-40. Epub 2010/12/21.

15. Cheon H, Stark GR. Unphosphorylated STAT1 prolongs the expression of interferon-induced immune regulatory genes. Proceedings of the National Academy of Sciences of the United States of America. 2009;106(23):9373-8. Epub 2009/05/30.

16. Khodarev NN, Beckett M, Labay E, Darga T, Roizman B, Weichselbaum RR. STAT1 is overexpressed in tumors selected for radioresistance and confers protection from radiation in transduced sensitive cells. Proc Natl Acad Sci U S A. 2004;101(6):1714-9. Epub 2004/02/03.

17. Tsai MH, Cook JA, Chandramouli GV, DeGraff W, Yan H, Zhao S, et al. Gene expression profiling of breast, prostate, and glioma cells following single versus fractionated doses of radiation. Cancer Res. 2007;67(8):3845-52. Epub 2007/04/19.

18. Haybaeck J, Obrist P, Schindler CU, Spizzo G, Doppler W. STAT-1 expression in human glioblastoma and peritumoral tissue. Anticancer research. 2007;27(6B):3829-35. Epub 2008/01/30.

19. Sgorbissa A, Tomasella A, Potu H, Manini I, Brancolini C. Type I IFNs signaling and apoptosis resistance in glioblastoma cells. Apoptosis : an international journal on programmed cell death. 2011;16(12):1229-44. Epub 2011/08/23.

20. Duarte CW, Willey CD, Zhi D, Cui X, Harris JJ, Vaughan LK, et al. Expression signature of IFN/STAT1 signaling genes predicts poor survival outcome in glioblastoma multiforme in a subtype-specific manner. PloS one. 2012;7(1):e29653. Epub 2012/01/14.

21. Gladson CL. The extracellular matrix of gliomas: modulation of cell function. Journal of neuropathology and experimental neurology. 1999;58(10):1029-40. Epub 1999/10/09.

22. Rubenstein BM, Kaufman LJ. The role of extracellular matrix in glioma invasion: a cellular Potts model approach. Biophysical journal. 2008;95(12):5661-80. Epub 2008/10/07.

23. Aguilar LK, Arvizu M, Aguilar-Cordova E, Chiocca EA. The spectrum of vaccine therapies for patients with glioblastoma multiforme. Curr Treat Options Oncol. 2012;13(4):437-50. Epub 2012/08/21.

24. Gatson NN, Chiocca EA, Kaur B. Anti-angiogenic gene therapy in the treatment of malignant gliomas. Neurosci Lett. 2012;527(2):62-70. Epub 2012/08/22.

25. Guo D, Reinitz F, Youssef M, Hong C, Nathanson D, Akhavan D, et al. An LXR agonist promotes glioblastoma cell death through inhibition of an EGFR/AKT/SREBP-1/LDLR-dependent pathway. Cancer Discov. 2011;1(5):442-56. Epub 2011/11/08.

FIGURE CAPTIONS

Figure 1. Gliomaspheres generated in air/liquid interface form a tumor-like tissue in vitro (A) GIC are forming gliomaspheres in culture (B) Gliomaspheres culture on air/liquid interface in neural induction medium at day 1. (C) 24 hours after plating on the membrane, gliomaspheres have merged. (D) Hemalun/eosin coloration of the obtained tissue after two weeks culture on air/liquid interface. (E, F) Immunostaining of histological sections derived from gliomaspheres plated on membrane for two weeks with the glial / neuronal markers GFAP, vimentin, nestin and βIII-tubulin.

Figure 2. . Gliomaspheres can generate a tumor-like tissue developing within non-tumoral nervous tissue *in vitro*. (A) Scheme of the experimental setup: ESC colonies were maintained as small suspension aggregates in neural induction medium for 4 days before plating on air/liquid interface cell culture system. After three weeks, aggregates merged and generated a neural tissue (ENT). At this stage, a few TFP-expressing gliomaspheres were placed on the ENT. Using florescent microscopy, a TFP positive area could be observed 14 days after culture (C) TFP-positive area 14 days after co-culture of gliomaspheres with ENT. (D) Higher magnification of a TFP-positive area 14 days after co-culture of gliomaspheres with ENT, showing cells with a neuritic morphology (E) TFP positive single cells distant from the main TFP-positive areas. (F) Hemalun/eosin histological coloration of gliomaspheres developing within ENT. (G-K) Several glial and neural markers known to be expressed in glioblastoma were analysed on co-culture sections: nestin, GFAP, vimentin, Musashi-1 and Sox-2.

Figure 3. Specific features of glioblastoma *in vivo* are mimicked *in vitro*. (A): Histological section (10µm) of the tissue two weeks after gliomasphere/ENT co-culture. (B) Invasion of ENT by TFP-positive glioblastoma cells. Histological sections and immuno fluorescent staining against GFAP were performed at different time points. (C) Histological section showing a secondary site distant from the main TFP-positive cells mass. (D) Lower magnification of a histological section showing secondary TFP-positive tumor foci distant from the main TFP-positive cell mass. (E) Immunohistochemistry against α-crytallin B in a section of gliomaspheres developing within ENT. (F) Hemalun/eosin histological coloration showing a necrotic area including picnotic nucli (black arrow) and (G) immunoreactivity for cleaved caspase-3.

Figure 4. Breast carcinoma and melanoma tumor cell co-culture on engineered neural tissue. (A) Scheme of the experimental setup. ENT were co-cultured with TFP-positive MCF-7 / MZ2-mel3.1 spheres for two weeks. (B) Histological section of the co-culture indicates the TFP expressing cells on the top of the ENT without massive single cell invasion into ENT. (C) The mammospheres which are at the upper part of the co-culture tissue were

positive for cytokeratins , shown more precisely (D) with higher magnification. (E) In contrast to gliomaspheres (GB1), TFP-positive MZ2-mel3.1 melanoma cells did not infiltrate ENT.

Figure 5. Glioblastoma/nervous tissue interaction induces transcriptional changes. (A) Scheme of the experimental setup (B) Comparative heatmap analysis showing gene expression profile of the four conditions described in (A): Each experimental condition was performed in biological triplicates and submitted to whole transcriptomea analysis using microarray.Red box upregulated gene; Blue box= downregulated gene. The name of each gene is shown on the right side of the heatmap with the Ilumina ID number. (C) Scatterplots illustrates differentially expressed genes due to co-culture of gliomaspheres on ENT. Genes involved in type I interferon response immune response are represented by red dots).

Figure 6. IFN responsive gene expression in gliomaspheres versus MCF-7 mammosphere co-cultured with ENT. (A, B) Q-PCR analysis was performed for a panel of IFN responsive genes with gliomasphere (A) or mammospheres (B) co-cultured with ENT for two weeks.

Figure 7. **Differentially expressed genes have a significant effect on patient survival**. (A) Interferon response, extracellular matrix and cholesterol metabolism-related genes up-regulated by the tumor/host tissue interaction. All genes in each group are ordered according to the fold change, shown on the left part of the x-axis (twelve genes have two rows, one for each Illumina probe). Effect on survival is shown on the right part of the x-axis. Threshold for significant effect on patient survival by Wald test scores is marked with a vertical dashed line. (B) For all the genes (ordered by fold change), the proportion of genes having significant Wald test score was calculated. It was done in a sliding window of 100 genes with overlap of 25 genes to show the change of survival effect related to fold change. Empirical p-values from 100 000 random sampling groups are shown with horizontal dashed lines. Windows where at least one gene had significant fold change are colored orange and turquoise for up-regulation and down-regulation, respectively. The trend line in blue shows smoothed signal from the proportion of survival affected genes

Supplementary Figure 1. Scatterplots demonstration of differentially expressed genes due to culture of gliomaspheres on air/liquid interface. Proliferation-associated genes are represented by blue dots (Full list of the genes available in Supplementary File 1).

Supplementary Figure 2. Network analysis of Microarray data comparison of ENT versus ENT+GB1 by using g:profiler software. Most of the genes up-regulated in ENT vs.ENT+GB1 were belonging to the IFN type I pathway. The colours of the lines are indicating the source of information's.

Supplementary Table 1. Co-culture of gliomaspheres from different patients with ENT.

Several gliomaspheres were derived *in vitro* after dissociation of surgical pieces of glioblastomas or glioneuronal tumors from different patients. The growth and invasion on ENT was evaluated on histological sections by immunofluorescent staining against GFAP.

Tumor sphere	Origin	Growth on ENT	Invasion of ENT
NS688	Glioblastoma	Low	-
NS711	Glioblastoma	+	+
NS713	Glioblastoma	+	+
GB1	Glioblastoma	+	+
TG1	Glioneuronal tumor	+	+
TG6	Glioneuronal tumor	Low	-
MCF7	Breast cancer	+	-
MZ2-mel3.1	melanoma	+	-

Supplementary table 2. Primers used for IFN responsive genes by quantitative PCR

Gene	Sense	Antisense
MX-1	GGGAAGGAATGGGAATCAGT	CCCACAGCCACTCTGGTTAT
OAS-1	CAAGCTCAAGAGCCTCATCC	TGGGCTGTGTTGAAATGTGT
OAS-2	GGTGAACACCATCTGTGACG	TACCATCGGAGTTGCCTCTT
OAS-3	GTCAAACCCAAGCCACAAGT	GGGCGAATGTTCACAAAGTT
IFIT-3	GGGCAGACTCTCAGATGCTC	CAGTTGTGTCCACCCTTCCT
DHX-58	CACAGGGAGCACGTCACTAA	ATTCTCTGGGCCATGAGTTG
C1QB	CCTTCTCTGCCACAAGAACC	CGGGGCTCATAATTGTTGTT
FCER1G	GGAGAGCCTCAGCTCTGCTA	CCTTTCGCACTTGGATCTTC
GAPDH	TTTGGTTGAGCACAGGGTACT	GAGATCCCTCCAAAATCAAGTG

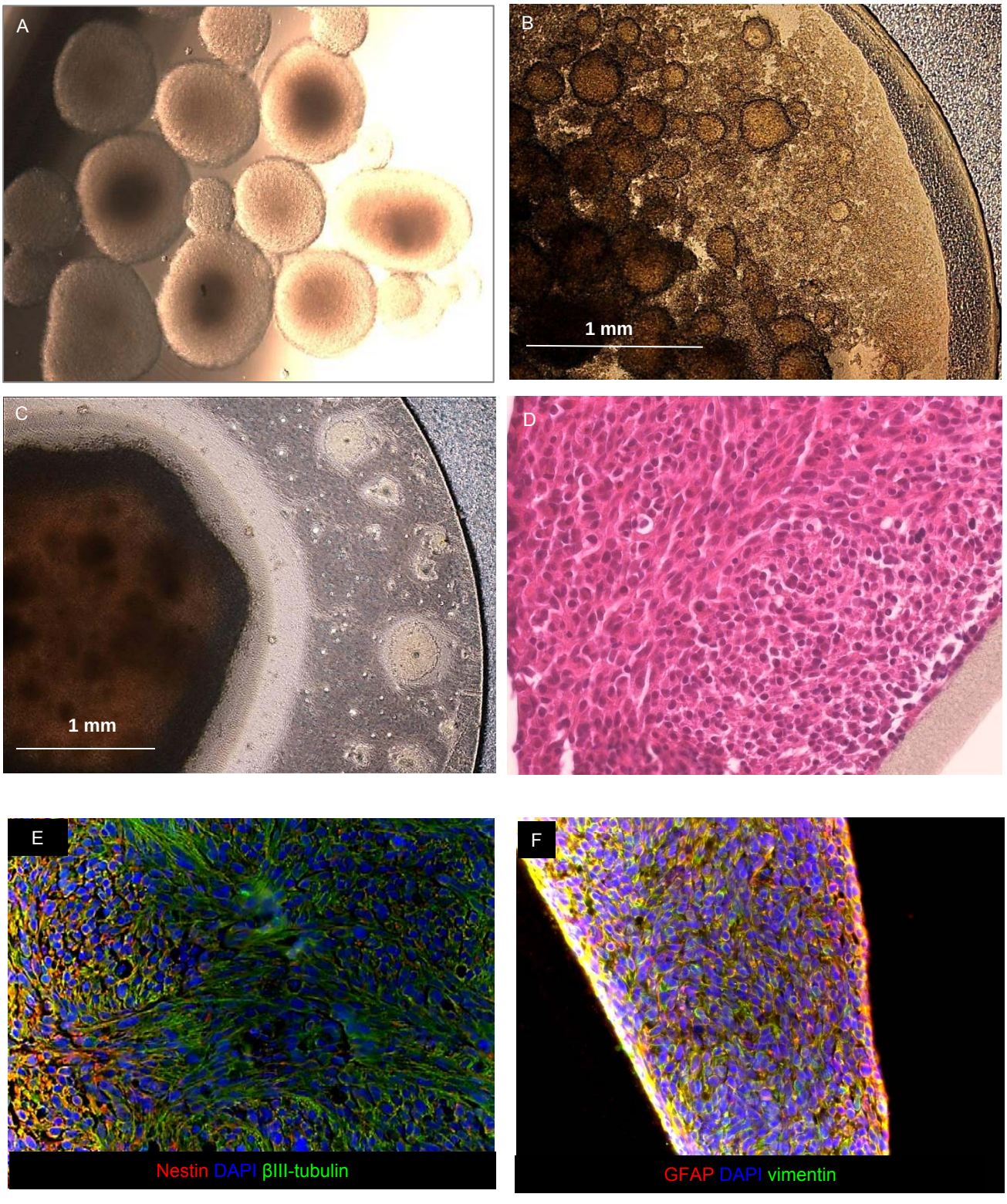

Figure 1

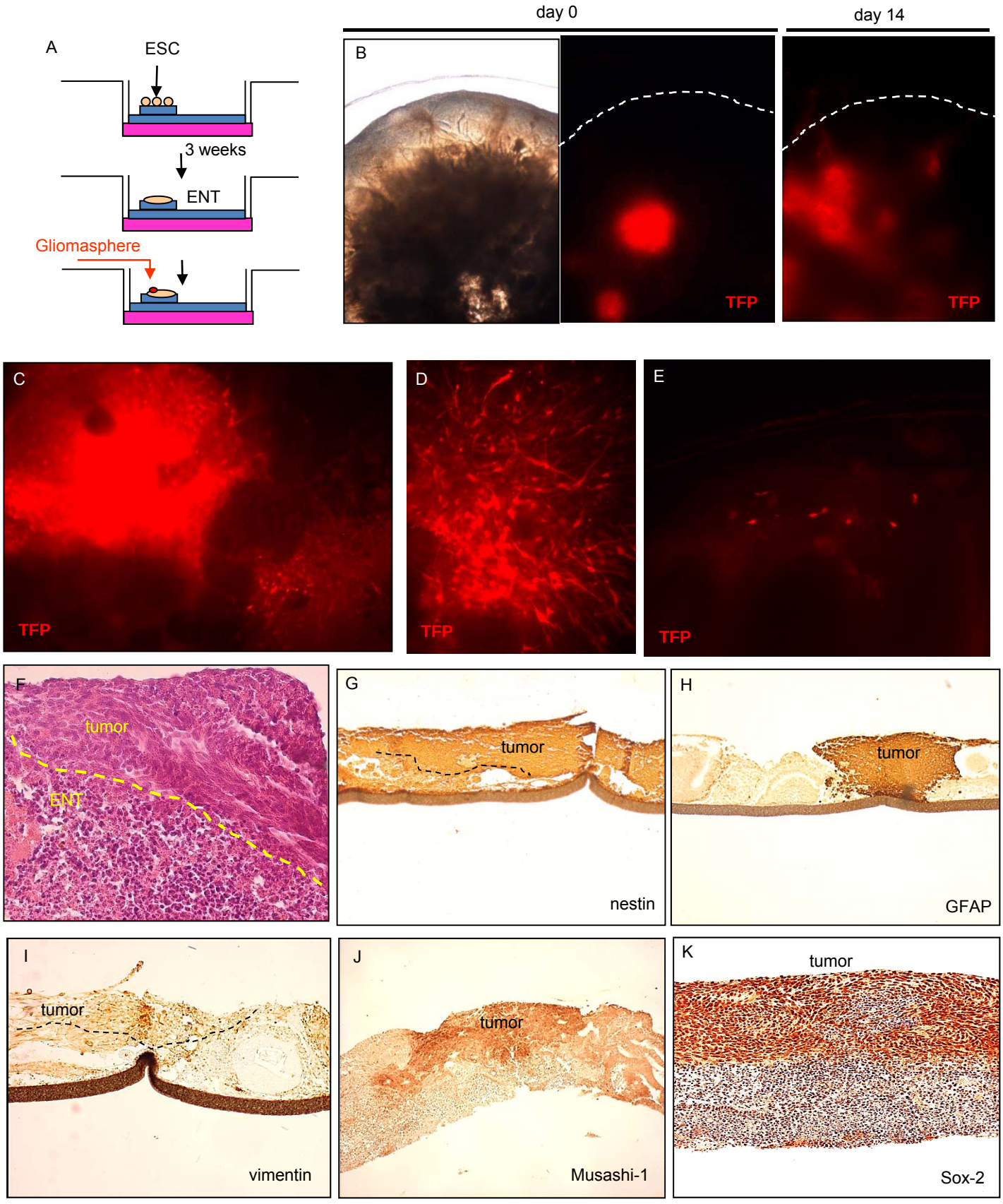
A
ESC
3 weeks
ENT
Gliomasphere
day 0
day 14
B
TFP
TFP
C
TFP
D
TFP
E
TFP
F
tumor
ENT
G
tumor
nestin
H
tumor
GFAP
I
tumor
vimentin
J
tumor
Musashi-1
K
tumor
Sox-2

Figure 2

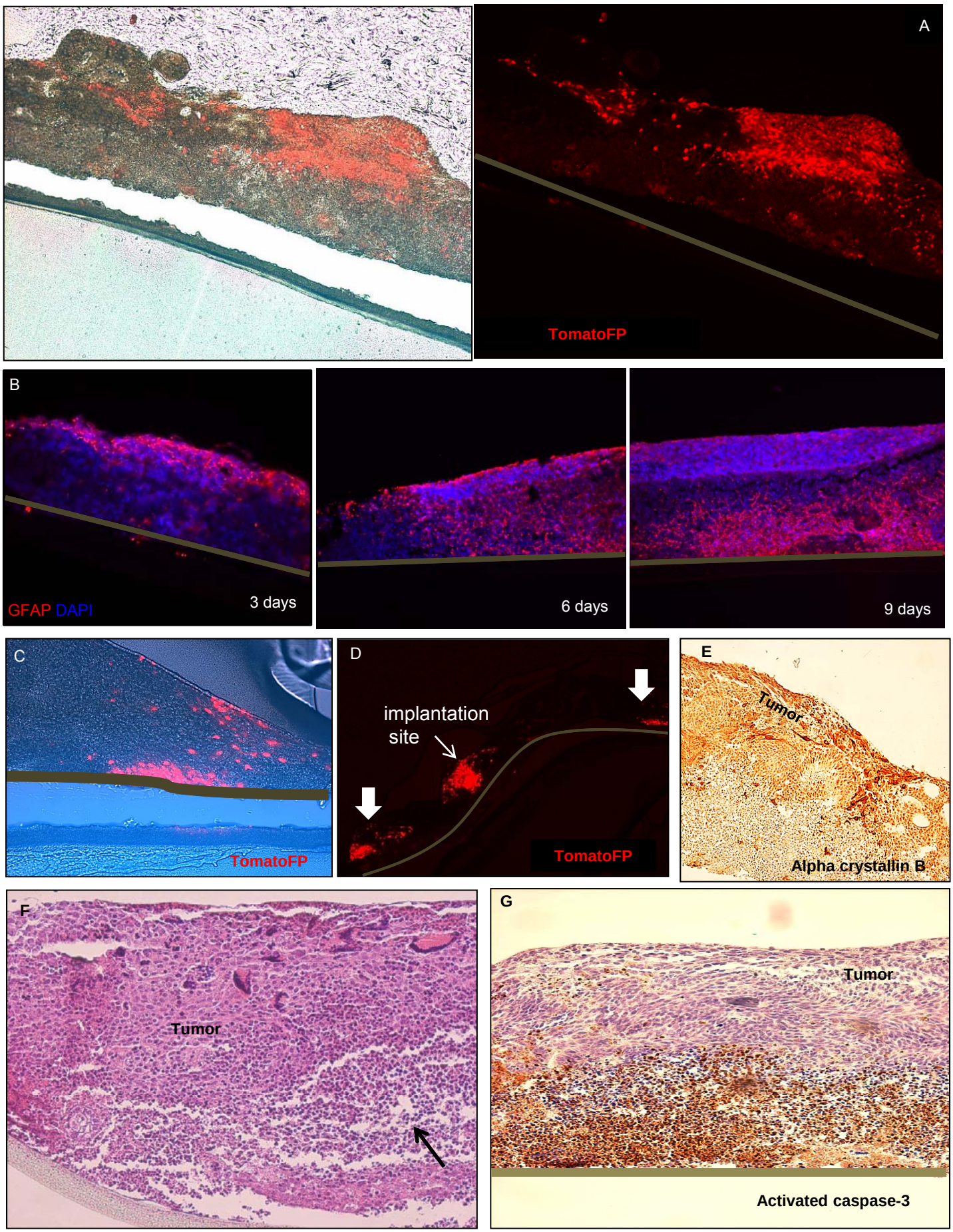
A
TomatoFP
B
GFAP DAPI
3 days
6 days
9 days
C
TomatoFP
D
implantation
site
TomatoFP
E
Tumor
Alpha crystallin B
F
Tumor
G
Tumor
Activated caspase-3

Figure 3

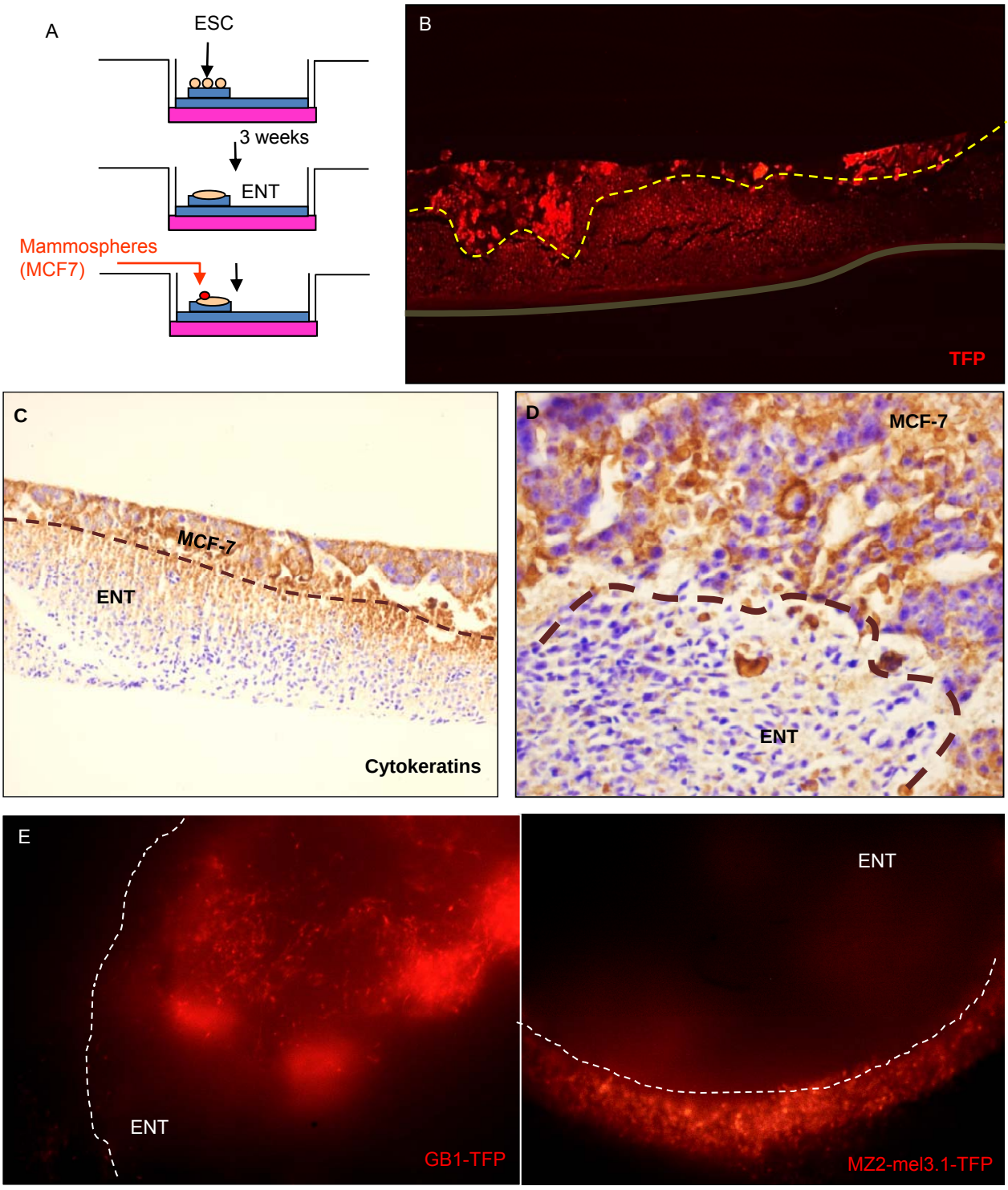
A
ESC
3 weeks
ENT
Mammospheres
(MCF7)
B
TFP
C
MCF-7
ENT
Cytokeratins
D
MCF-7
ENT
E
ENT
GB1-TFP
ENT
MZ2-mel3.1-TFP

Figure 4

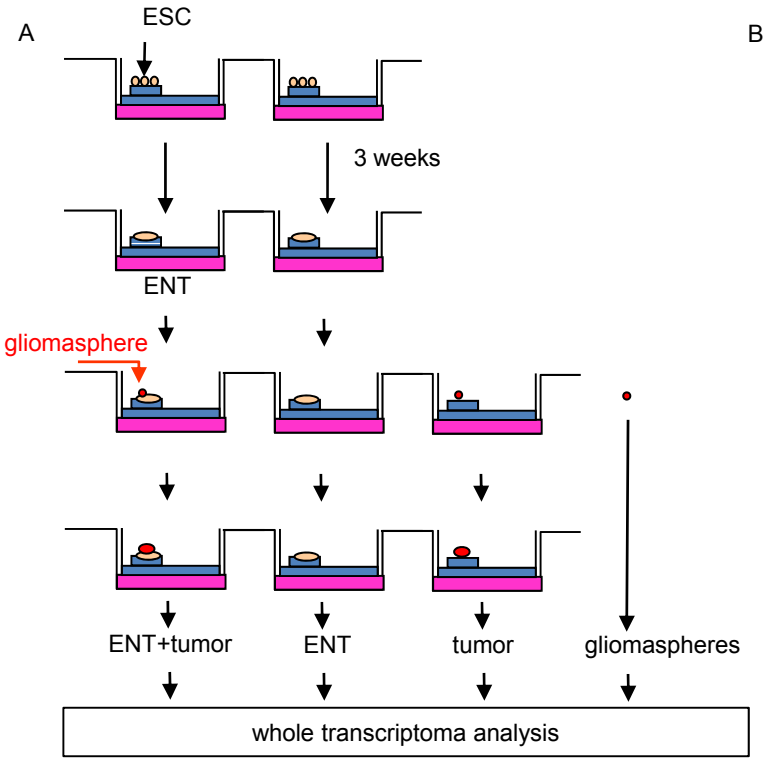
A
ESC
3 weeks
ENT
gliomasphere
ENT+tumor
ENT
tumor
gliomaspheres
whole transcriptoma analysis

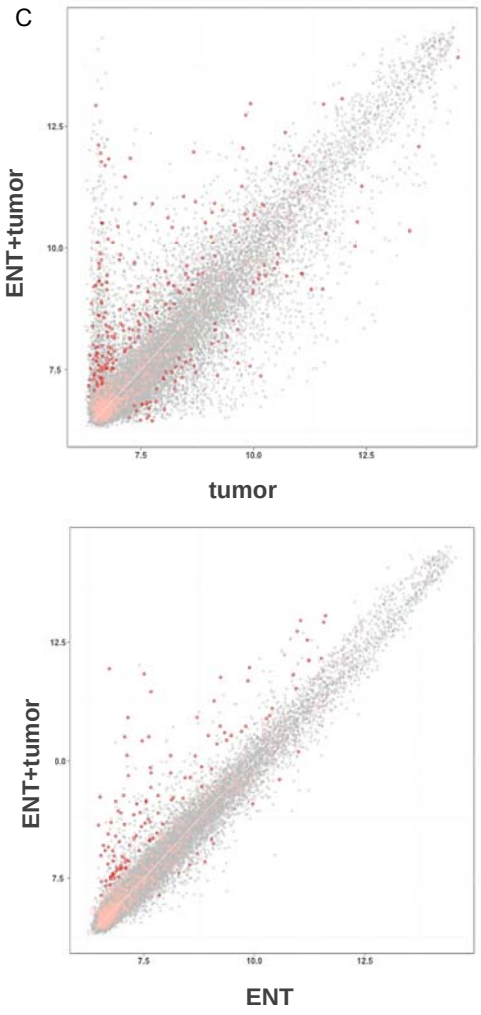
C
ENT+tumor
tumor
ENT+tumor
ENT

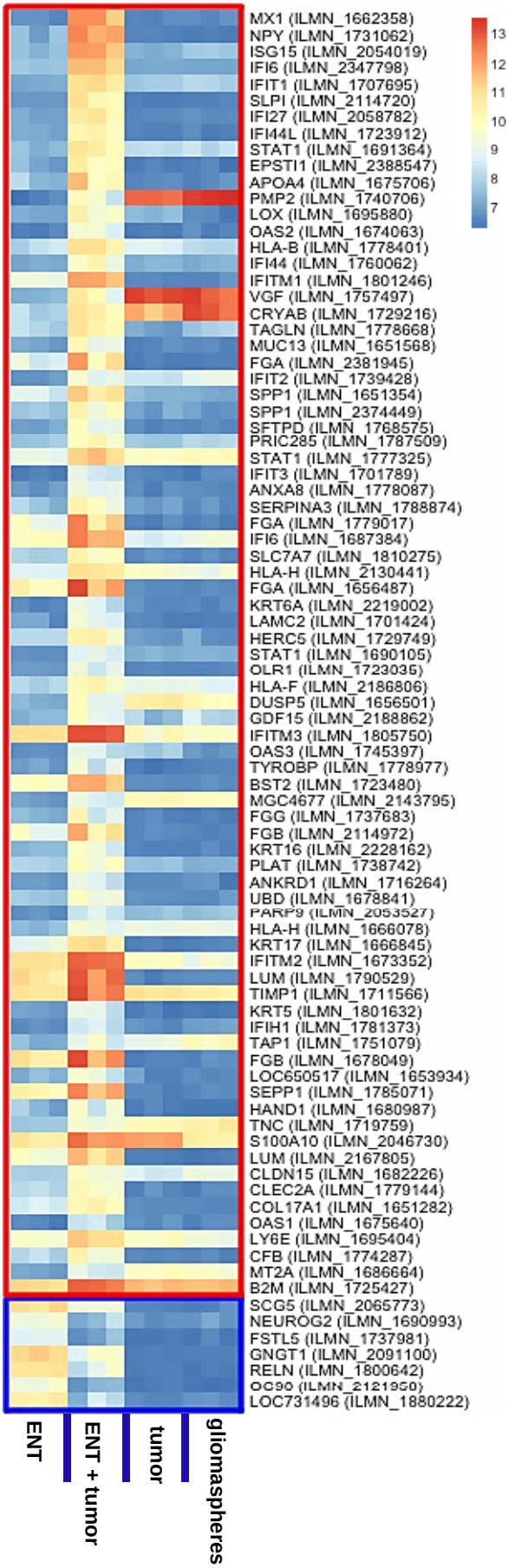
B
MX1 (ILMN_1662358)
NPY (ILMN_1731062)
ISG15 (ILMN_2054019)
IFI6 (ILMN_2347798)
IFIT1 (ILMN_1707695)
SLPI (ILMN_2114720)
IFI27 (ILMN_2058782)
IFI44L (ILMN_1723912)
STAT1 (ILMN_1691364)
EPSTI1 (ILMN_2388547)
APOA4 (ILMN_1675706)
PMP2 (ILMN_1740706)
LOX (ILMN_1695880)
OAS2 (ILMN_1674063)
HLA-B (ILMN_1778401)
IFI44 (ILMN_1760062)
IFITM1 (ILMN_1801246)
VGF (ILMN_1757497)
CRYAB (ILMN_1729216)
TAGLN (ILMN_1778668)
MUC13 (ILMN_1651568)
FGA (ILMN_2381945)
IFIT2 (ILMN_1739428)
SPP1 (ILMN_1651354)
SPP1 (ILMN_2374449)
SFTPD (ILMN_1768575)
PRIC285 (ILMN_1787509)
STAT1 (ILMN_1777325)
IFIT3 (ILMN_1701789)
ANXA8 (ILMN_1778087)
SERPINA3 (ILMN_1788874)
FGA (ILMN_1779017)
IFI6 (ILMN_1687384)
SLC7A7 (ILMN_1810275)
HLA-H (ILMN_2130441)
FGA (ILMN_1656487)
KRT6A (ILMN_2219002)
LAMC2 (ILMN_1701424)
HERC5 (ILMN_1729749)
STAT1 (ILMN_1690105)
OLR1 (ILMN_1723035)
HLA-F (ILMN_2186806)
DUSP5 (ILMN_1656501)
GDF15 (ILMN_2188862)
IFITM3 (ILMN_1805750)
OAS3 (ILMN_1745397)
TYROBP (ILMN_1778977)
BST2 (ILMN_1723480)
MGC4677 (ILMN_2143795)
FGG (ILMN_1737683)
FGB (ILMN_2114972)
KRT16 (ILMN_2228162)
PLAT (ILMN_1738742)
ANKRD1 (ILMN_1716264)
UBD (ILMN_1678841)
PARP9 (ILMN_2053527)
HLA-H (ILMN_1666078)
KRT17 (ILMN_1666845)
IFITM2 (ILMN_1673352)
LUM (ILMN_1790529)
TIMP1 (ILMN_1711566)
KRT5 (ILMN_1801632)
IFIH1 (ILMN_1781373)
TAP1 (ILMN_1751079)
FGB (ILMN_1678049)
LOC650517 (ILMN_1653934)
SEPP1 (ILMN_1785071)
HAND1 (ILMN_1680987)
TNC (ILMN_1719759)
S100A10 (ILMN_2046730)
LUM (ILMN_2167805)
CLDN15 (ILMN_1682226)
CLEC2A (ILMN_1779144)
COL17A1 (ILMN_1651282)
OAS1 (ILMN_1675640)
LY6E (ILMN_1695404)
CFB (ILMN_1774287)
MT2A (ILMN_1686664)
B2M (ILMN_1725427)
SCG5 (ILMN_2065773)
NEUROG2 (ILMN_1690993)
FSTL5 (ILMN_1737981)
GNGT1 (ILMN_2091100)
RELN (ILMN_1800642)
OC90 (ILMN_2121950)
LOC731496 (ILMN_1880222)
13
12
11
10
9
8
7
ENT
ENT + tumor
tumor
gliomaspheres

Figure 5

A

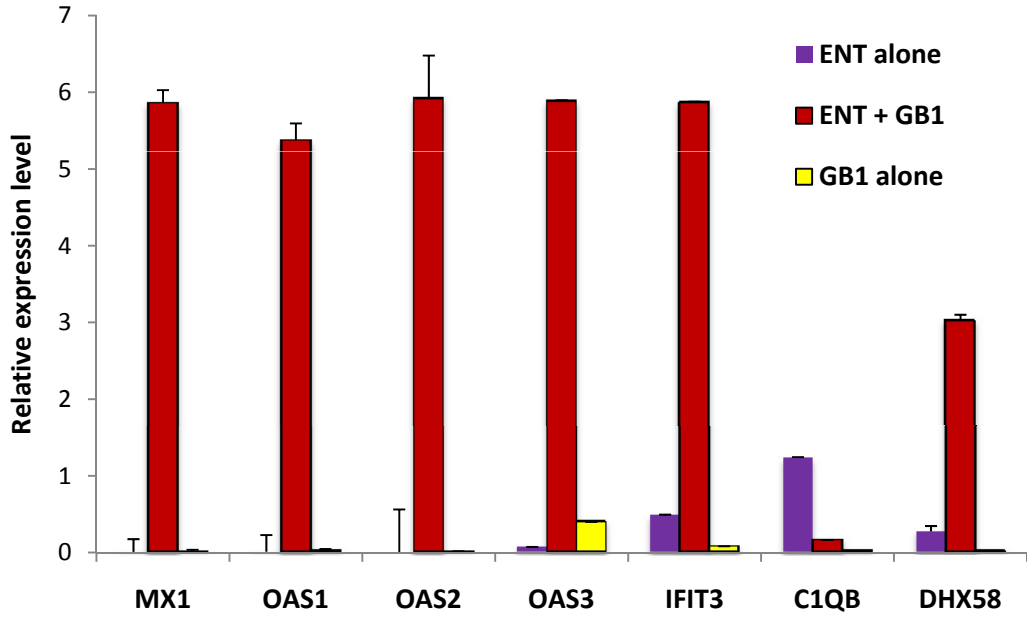
Relative expression level
7
6
5
4
3
2
1
0
ENT alone
ENT + GB1
GB1 alone
MX1
OAS1
OAS2
OAS3
IFIT3
C1QB
DHX58

B

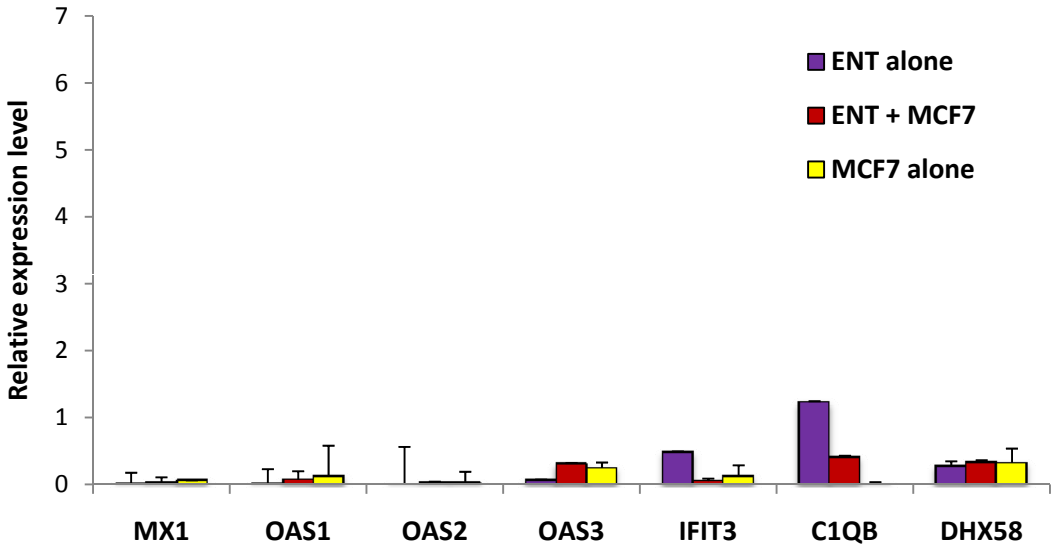
Relative expression level
7
6
5
4
3
2
1
0
ENT alone
ENT + MCF7
MCF7 alone
MX1
OAS1
OAS2
OAS3
IFIT3
C1QB
DHX58

Figure 6

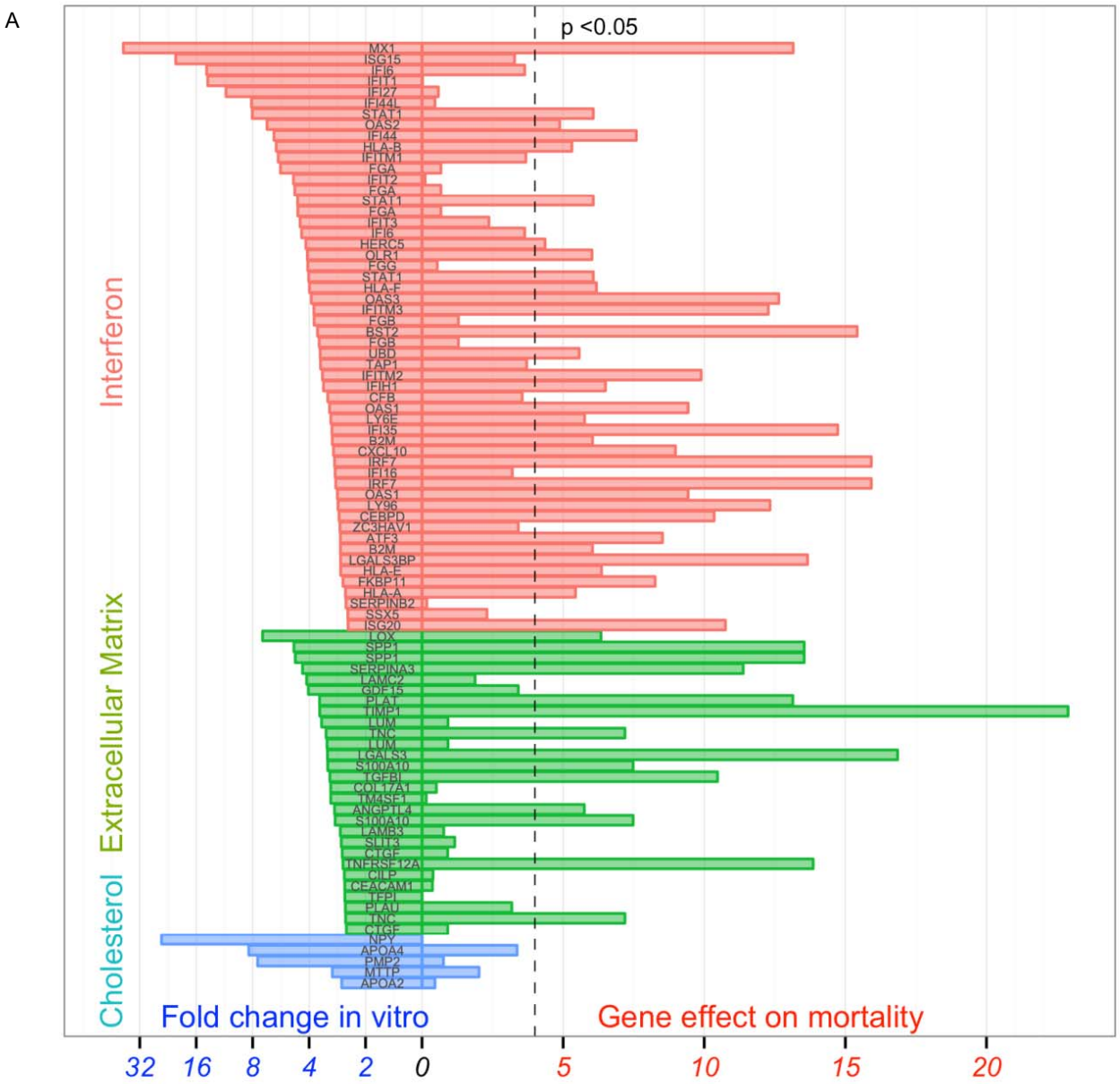
A
p <0.05
Interferon
Extracellular Matrix
Cholesterol
MX1
ISG15
IFI6
IFIT1
IFI27
IFI44L
STAT1
OAS2
IFI44
HLA-B
IFITM1
FGA
IFIT2
FGA
STAT1
FGA
IFIT3
IFI6
HERC5
OLR1
FGG
STAT1
HLA-F
OAS3
IFITM3
FGB
BST2
FGB
UBD
TAP1
IFITM2
IFIH1
CFB
OAS1
LY6E
IFI35
B2M
CXCL10
IRF7
IFI16
IRF7
OAS1
LY96
CEBPD
ZC3HAV1
ATF3
B2M
LGALS3BP
HLA-E
FKBP11
HLA-A
SERPINB2
SSX5
ISG20
LOX
SPP1
SPP1
SERPINA3
LAMC2
GDF15
PLAT
TIMP1
LUM
TNC
LUM
LGALS3
S100A10
TGFBI
COL17A1
TM4SF1
ANGPTL4
S100A10
LAMB3
SLIT3
CTGF
TNFRSF12A
CILP
CEACAM1
TPI1
PLAU
TNC
CTGF
NPY
APOA4
PMP2
MTP
APOA2
Fold change in vitro
Gene effect on mortality
32
16
8
4
2
0
5
10
15
20
B
Percentage of genes having effect on mortality
50
40
30
20
10
0
p=1.0e-05
p=0.05
Increase (37.5)
none
Decrease (-1.83)
Fold change in vitro

Figure 7

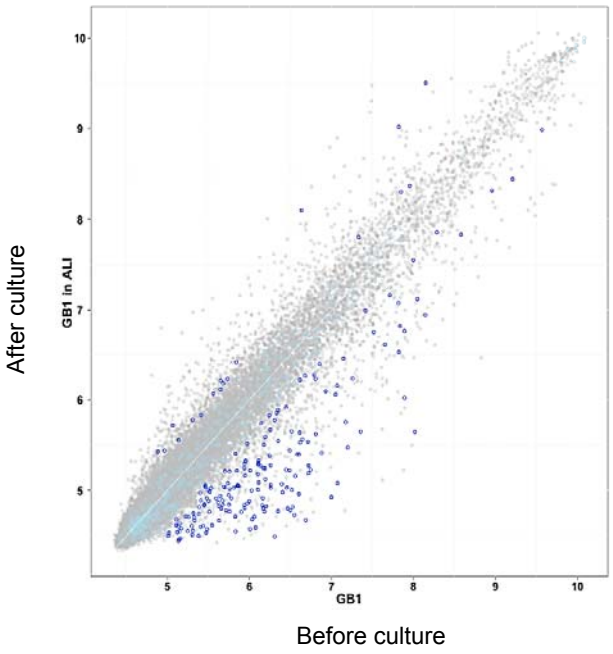

Supplementary figure 1

Supplementary figure 2